

Co-occurrence of Photochemical and Microbiological Transformation Processes in Open-Water Unit Process Wetlands

Carsten Prasse,^{†,‡} Jannis Wenk,^{†,§} Justin T. Jasper,[†] Thomas A. Ternes,[‡] and David L. Sedlak^{*,†}

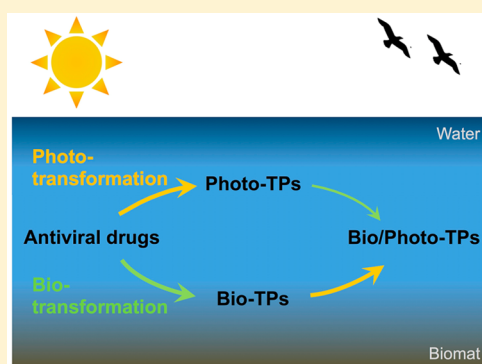
[†]ReNUWIt Engineering Research Center and Department of Civil & Environmental Engineering, University of California at Berkeley, Berkeley, California 94720, United States

[‡]Department of Aquatic Chemistry, Federal Institute of Hydrology, D-56002 Koblenz, Germany

[§]Department of Chemical Engineering and Water Innovation & Research Centre, University of Bath, Claverton Down, Bath BA2 7AY, United Kingdom

S Supporting Information

ABSTRACT: The fate of anthropogenic trace organic contaminants in surface waters can be complex due to the occurrence of multiple parallel and consecutive transformation processes. In this study, the removal of five antiviral drugs (abacavir, acyclovir, emtricitabine, lamivudine and zidovudine) via both bio- and phototransformation processes, was investigated in laboratory microcosm experiments simulating an open-water unit process wetland receiving municipal wastewater effluent. Phototransformation was the main removal mechanism for abacavir, zidovudine, and emtricitabine, with half-lives ($t_{1/2, \text{photo}}$) in wetland water of 1.6, 7.6, and 25 h, respectively. In contrast, removal of acyclovir and lamivudine was mainly attributable to slower microbial processes ($t_{1/2, \text{bio}} = 74$ and 120 h, respectively). Identification of transformation products revealed that bio- and phototransformation reactions took place at different moieties. For abacavir and zidovudine, rapid transformation was attributable to high reactivity of the cyclopropylamine and azido moieties, respectively. Despite substantial differences in kinetics of different antiviral drugs, biotransformation reactions mainly involved oxidation of hydroxyl groups to the corresponding carboxylic acids. Phototransformation rates of parent antiviral drugs and their biotransformation products were similar, indicating that prior exposure to microorganisms (e.g., in a wastewater treatment plant or a vegetated wetland) would not affect the rate of transformation of the part of the molecule susceptible to phototransformation. However, phototransformation strongly affected the rates of biotransformation of the hydroxyl groups, which in some cases resulted in greater persistence of phototransformation products.



INTRODUCTION

Discharge of municipal wastewater effluents into surface waters can result in the presence of trace organic contaminants at concentrations that pose potential risks to aquatic ecosystems and drinking water resources. After their release, many trace organic contaminants are attenuated by biological and photochemical processes. Although these processes often occur simultaneously or sequentially in the environment, most studies have considered the occurrence of only one transformation process at a time.^{1–4} Thus, it is difficult to predict which transformation products will be formed and whether or not transformation reactions occurring at one moiety alter the kinetics of subsequent transformation reactions. Furthermore, if partial transformation of a compound enhances the reactivity of other moieties, then interaction of transformation processes could result in changes in the distribution of transformation products as well as their rates of removal. For example, carbamazepine, a compound that is particularly resistant to biotransformation, is slowly transformed upon exposure to sunlight via direct photolysis and reaction with $\cdot\text{OH}$.^{5,6} This

leads to the formation of hydroxylated derivatives,⁷ which are more easily biodegraded than the parent compound.⁸

Open-water unit process wetlands have been developed as a polishing treatment step for municipal wastewater effluents.⁹ These managed natural systems utilize sunlight to remove trace organic compounds and inactivate pathogens.^{10–12} In addition, microorganisms in the biomat formed at the bottom of these treatment basins reduce nitrate and contribute to aerobic biodegradation of trace organic contaminants.^{13,14} To assess the importance of co-occurrence of biological and photochemical transformation reactions for reaction kinetics and product distribution, the fate of five antiviral drugs (abacavir, emtricitabine, lamivudine, zidovudine, and acyclovir; see Figure 1) was studied under conditions comparable to those encountered in open-water unit process wetlands.

Received: August 5, 2015

Revised: October 21, 2015

Accepted: October 28, 2015

Published: November 12, 2015

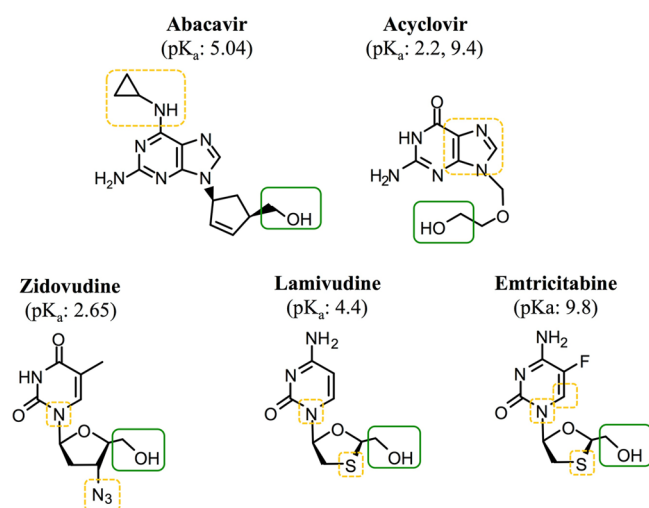


Figure 1. Antiviral drugs and their most likely sites of proposed phototransformation (outlined in orange) and biotransformation (outlined in green) reactions.

Antiviral drugs were chosen because they are widely used for the treatment of diseases such as herpes, hepatitis, and human immunodeficiency virus (HIV) and have been detected at concentrations above $1 \mu\text{g}\cdot\text{L}^{-1}$ in municipal wastewater effluents.^{15–18} No information about potential environmental effects resulting from the release of these compounds into the aquatic environment is available so far. Furthermore, little is known about the effects of these compounds on environmental viruses, a group of microorganisms that play a very important role in aquatic ecosystems.¹⁹

By investigating transformation kinetics and mechanisms under conditions comparable to those encountered in open-water unit process wetlands, it is possible to gain insight into how simultaneously occurring bio- and phototransformation reactions affect the overall fate of antiviral drugs in sunlit surface waters. These compounds also serve as models for other families of compounds that contain moieties susceptible to bio- and phototransformation.

MATERIALS AND METHODS

Chemicals. Analytical reference standards of antiviral drugs and stable isotope-labeled analogues used as internal standards (purity >99%) were purchased from Toronto Research Chemicals (Ontario, Canada). All other chemicals and solvents were obtained from Fisher Scientific (Fairlawn, NJ).

Wetland Water Sampling Conditions. Phototransformation experiments were conducted in water collected from a pilot-scale open-water unit process wetland located in Discovery Bay, CA. The facility treats about 10 000 gallons/day ($4.4 \times 10^{-4} \text{ m}^3\cdot\text{s}^{-1}$) of nitrified wastewater effluent from an adjacent municipal wastewater treatment plant. Details about the open-water unit process wetland were described previously.^{10,13} Water collected from the open-water wetland typically contained $10\text{--}20 \text{ mg}\cdot\text{N}\cdot\text{L}^{-1} \text{ NO}_3^-$, $5\text{--}10 \text{ mg}\cdot\text{C}\cdot\text{L}^{-1}$ dissolved organic carbon (DOC), and $60\text{--}80 \text{ mg}\cdot\text{C}\cdot\text{L}^{-1}$ dissolved inorganic carbon (HCO_3^- and CO_3^{2-}). Samples for laboratory irradiation experiments were collected from the midpoint of the wetland. All samples were filtered through prerinsed $1 \mu\text{m}$ (nominal pore size) glass fiber filters (Whatman) and were stored in the dark at 4°C until analysis, which occurred within 5 days.

Laboratory Photo- and Biotransformation Experiments. Irradiation experiments were performed by use of a collimated beam Oriel solar simulator (Spectra Physics 91194) equipped with a 1000 W Xe lamp and either two successive atmospheric attenuation filters (Spectra Physics 81088 and 81017) or one atmospheric and one UVB filter (Spectra Physics 81088 and 81050). Spectral irradiance was routinely measured with a spectroradiometer (RPS 380, international light) at different locations of the irradiated area to assess variability, which was always <5%. Details on lamp irradiance energies and the spectra of different configurations are given in section 1.1 of [Supporting Information](#). Irradiation experiments were carried out in 100 mL black-painted glass beakers that were placed in a water bath at constant temperature ($18 \pm 2^\circ\text{C}$). Initial concentrations of antivirals of approximately $0.5 \mu\text{M}$ were used for all kinetic experiments. Pseudo-first-order phototransformation rate constants of antivirals and photochemical probe compounds, used for quantification of concentrations of reactive intermediates, were calculated from the slopes of linear regression of the natural log of concentration versus time. No degradation of antiviral drugs was observed in control experiments in the dark, indicating that their transformation in filtered wetland water was attributable only to photochemical processes.

For the elucidation of biotransformation kinetics, beakers were additionally supplemented with 10 mL of the biotransformation taken from the bottom of a pilot-scale open-water wetland and kept in the dark (see Jasper et al.¹³ for further details). Biodegradation of compounds followed pseudo-first-order degradation kinetics, indicating stable conditions throughout the experiments. In addition, observed transformation rates were in good agreement with results from a preliminary study used to design the more detailed experiments.

Direct and Indirect Phototransformation. Experiments to assess direct phototransformation of antiviral drugs were conducted in buffered ultrapure water at pH values ranging from 6 to 10 (pH 6–8, 5 mM phosphate buffer; pH 9–10, 5 mM borate buffer). Samples (1 mL) were collected at regular time intervals and stored at 4°C in the dark until analysis. Electronic absorption spectra of antiviral drugs at different pH values (see [Figure S2](#)) were recorded with a UV-2600 UV-vis spectrophotometer (Shimadzu) using quartz-glass cuvettes (Hellma, Germany). Further details on determination of quantum yields by the *p*-nitroanisole (PNA)/pyridine (PYR) method²⁰ and related calculations are provided in section 1.7 of [Supporting Information](#).

Indirect phototransformation of antiviral drugs was investigated by the addition of specific quenchers to wetland water: *N,N*-dimethylaniline (DMA; $10 \mu\text{M}$) was used to scavenge CO_3^- radicals,¹⁰ sorbic acid (2.5 mM) was used to scavenge excited triplet states of the dissolved organic matter ($^3\text{DOM}^*$),²¹ histidine (20 mM) was used to scavenge singlet oxygen ($^1\text{O}_2$),²² and isopropyl alcohol (IPA; 26 mM) was used to scavenge $^{\bullet}\text{OH}$ radicals.²³ In addition, experiments with specific photosensitizers were conducted in ultrapure buffered water to determine reaction rate constants of antiviral drugs with individual reactive intermediates. For CO_3^- , either $\text{NaNO}_3/\text{NaHCO}_3$ or duroquinone/ NaHCO_3 photosensitizer method was used.^{24,25} Excited triplet state photosensitizers 3-methoxyacetophenone (3MAP) and anthraquinone-2-sulfonate (AQ2S) served as proxies for $^3\text{DOM}^*$.²⁶ Hydroxyl radicals were generated by irradiation of NaNO_3 solutions.²⁷ For $^1\text{O}_2$ production, rose bengal was used as a photosensitizer.²⁸ To

further verify the role of $^1\text{O}_2$, some experiments were performed in D_2O . Reaction rate constants were determined either by competition kinetics or by comparing reaction rates of antiviral drugs with those of established photochemical probe compounds (experimental details and calculations are provided in Supporting Information sections 1.5 and 1.6). For all indirect phototransformation experiments, the concentration changes of photochemical probe compounds and antiviral drugs during irradiation were determined by HPLC-UV. Experimental and analytical details, including comprehensive results, are provided in Supporting Information section 1.2.

Given the structural similarities of antivirals with DNA bases, additional irradiation experiments were performed with adenine, 2-aminoadenosine, cytosine, cytidine, guanine, thymidine, and thymine (Supporting Information section 2.1.1) to obtain further information about photoreactive moieties in the molecules to aid in identification of transformation products.

Identification of Photo- and Biotransformation Products. High-resolution mass spectrometry (HRMS; LTQ Orbitrap Velos, Thermo Scientific, Bremen, Germany) was used to conduct accurate MS and MS/MS analysis of transformation products of antiviral drugs. To this end, experiments at elevated concentrations ($40\text{ }\mu\text{M}$) were used. The LTQ Orbitrap Velos was coupled to a Thermo Scientific Accela liquid chromatography system (Accela pump and autosampler). HRMS was conducted in the positive electrospray ionization (ESI) mode. To obtain information on the chemical structure of transformation products, MSⁿ fragmentation experiments were conducted with data-dependent acquisition. Further information on the applied setup and data-dependent acquisition parameters can be found in Supporting Information (section 1.3). Product formation of antiviral drugs in laboratory experiments was determined by liquid chromatography/tandem mass spectrometry (LC/MS/MS). Details are provided in Supporting Information (section 1.4).

Combined Bio- and Photodegradation Experiments. The fate of antiviral drugs in the presence of sunlight and microorganisms was investigated over a 72 h period in the laboratory. Black-painted glass beakers (250 mL) were filled with 180 mL of wetland water and 20 mL of freshly collected biomat material from the bottom of the Discovery Bay open-water unit process wetland. The experimental setup was the same as described above for photochemical experiments but with three day/night cycles to simulate field conditions (8 h of daily irradiation followed by 16 h of darkness; 72 h total). Antiviral drugs were added individually at concentrations of approximately $0.5\text{ }\mu\text{M}$ to ensure detection of both parent antiviral compounds and their transformation products. Samples were collected at regular time intervals and stored at $4\text{ }^\circ\text{C}$ in the dark prior to LC/MS/MS analysis, which occurred within 24 h. Further details about the analytical method can be found in Supporting Information.

RESULTS AND DISCUSSION

Phototransformation in Wetland Water. Phototransformation of the five investigated antiviral drugs in wetland water followed first-order kinetics ($r^2 \geq 0.98$; Figures S4–S8). In native wetland water (pH 8.9), the fastest phototransformations were observed for abacavir ($k_{\text{obs}} = 0.52 \pm 0.06\text{ h}^{-1}$), zidovudine ($k_{\text{obs}} = 0.09 \pm 0.002\text{ h}^{-1}$) and emtricitabine ($k_{\text{obs}} = 0.03 \pm 0.002\text{ h}^{-1}$) whereas the transformations of acyclovir and lamivudine were significantly slower ($k_{\text{obs}} = 0.012 \pm 0.001$ and $0.011 \pm 0.001\text{ h}^{-1}$, respectively) (Figure 2). No

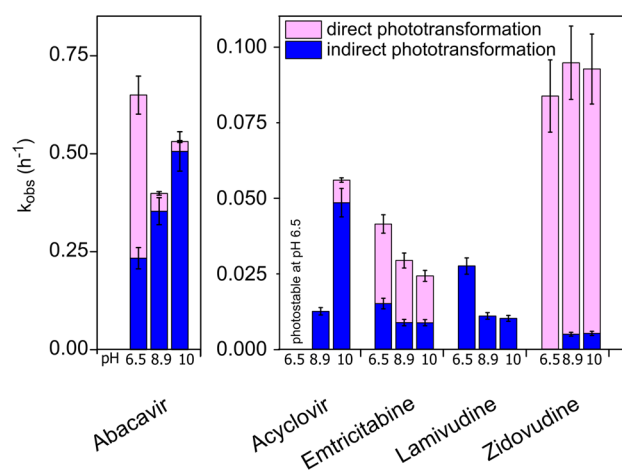


Figure 2. Phototransformation kinetics of antiviral drugs in experiments with wetland water at different pH values and contribution of direct and indirect photolysis processes by comparison with results obtained in ultrapure water. Data for wetland water are corrected for light absorption. Error bars show 95% confidence intervals.

degradation of antiviral drugs in wetland water occurred in the dark, indicating that their removal was solely attributable to photochemical processes. Photosynthetic activity leads to significant diurnal fluctuations of pH in open-surface wetlands.¹⁰ Therefore, phototransformation kinetics of antiviral drugs in wetland water were also determined at pH 6.5 and 10 (Figure 2).

Phototransformation of abacavir in wetland water increased when the pH value was adjusted to 6.5 or 10. This can be attributed to a higher contribution of direct photolysis due to higher quantum yields at lower pH values (i.e., Φ_{app} is 4.2–11.4 times higher between pH 6 and 8 compared to pH 9 and 10; Table S5) and faster indirect photolysis at higher pH values. Comparison of transformation kinetics with results obtained in ultrapure water revealed the dominance of indirect photodegradation processes at pH 8.9 and 10, whereas direct photolysis was more important at pH 6.5. The addition of sorbic acid and histidine significantly reduced phototransformation rates of abacavir in wetland water (Figure S4). Although interpretation of results from experiments with scavengers requires caution,²⁹ these results suggest the involvement of $^3\text{DOM}^*$ and $^1\text{O}_2$ in the photochemical fate of this compound. This was also supported by experiments with specific singlet oxygen and excited triplet state sensitizers (see below). Negligible removal of the structural analogues adenine and 2-aminoadenosine further indicated that the photolability of abacavir can be attributed to the cyclopropyl moiety (see Supporting Information section 2.1.1).

Rates of phototransformation of zidovudine were not affected by changes in pH. Comparison with reaction rates in both ultrapure water and wetland water in the presence of scavengers revealed the dominance of direct photolysis (Figure S5). Similar to abacavir, comparison with the depletion of structural analogues thymine and thymidine indicated that the azide moiety was responsible for the observed photoreactivity of zidovudine, as both analogues showed no removal when exposed to light (see Supporting Information section 2.1.1).

Phototransformation rates of acyclovir in wetland water increased with increasing pH. Comparison with results from ultrapure water revealed that removal at pH 8.9 was solely due to indirect photolysis, whereas at pH 10 direct photolysis was

Table 1. Quantum Yields (pH 9) and Apparent Second-Order Reaction Rate Constants of Indirect Phototransformation of Antiviral Drugs^a

	$\Phi_{\text{app}}(300-400\text{nm})$ at pH 9 ($\text{M}^{-1}\text{einstein}^{-1}$)	apparent second-order reaction rate constants ($\text{M}^{-1}\text{s}^{-1}$)					³ Sens* (AQ2S)	³ Sens* (MAP)
		$^1\text{O}_2$	$\bullet\text{OH}$	$\bullet\text{CO}_3^-$ ($\text{NO}_3^- + \text{HCO}_3^-/\text{CO}_3^{2-}$)	$\bullet\text{CO}_3^-$ (DQ)			
abacavir	0.014 (± 0.003)	1.2×10^9 ($\pm 18\%$)	1.1×10^{11} ($\pm 3\%$)	1.2×10^9 ($\pm 4\%$)	— ^b		4.88	13.5
zidovudine	0.45 (± 0.15)	ND ^c	1.3×10^{10} ($\pm 2\%$)	2.4×10^6 ($\pm 5\%$)	1.3×10^6 ($\pm 4\%$)		0.62	ND
acyclovir	0.01 (± 0.005)	1.2×10^7 ($\pm 25\%$)	5.0×10^9 ($\pm 2\%$)	1.2×10^8 ($\pm 2\%$)	6.3×10^7 ($\pm 4\%$)		0.08	ND
emtricitabine	0.016 (± 0.005)	ND	9.3×10^9 ($\pm 2\%$)	3.0×10^6 ($\pm 4\%$)	4.3×10^6 ($\pm 12\%$)		2.03	ND
lamivudine	ND	ND	9.2×10^9 ($\pm 1\%$)	1.2×10^6 ($\pm 3\%$)	1.7×10^6 ($\pm 3\%$)		1.86	ND

^aIndirect phototransformation occurred via reaction with $^1\text{O}_2$, $\bullet\text{OH}$, $\bullet\text{CO}_3^-$, and excited triplet states (values are given relative to degradation of the ³Sens* probe compound TMP). Quantum yields of antiviral drugs at pH 6–8 and pH 10 can be found in Table S5. ^bNot applicable due to reaction of abacavir with DQ in the dark. ^cND, not detected above the level of uncertainty.

also important. Significantly reduced rates of acyclovir phototransformation in the presence of histidine and sorbic acid indicated the importance of $^1\text{O}_2$ and ³DOM* to indirect photolysis (Figure S6). In contrast to abacavir and zidovudine, phototransformation kinetics were similar to those observed for the structural analogue guanine (Figure S15). Thus, phototransformation of acyclovir can be attributed primarily to the guanine moiety.

For lamivudine and emtricitabine, phototransformation kinetics in wetland water decreased with increasing pH. No removal of lamivudine was observed in ultrapure water, indicating that its removal was entirely attributable to indirect photolysis. Higher phototransformation rates of emtricitabine relative to lamivudine further indicated the strong influence of the fluorine atom for emtricitabine's photolability. The presence of the fluorine substituent led to greater light absorption at 300–320 nm (Figure S2). Even though the absorption spectrum of emtricitabine did not change with pH, the quantum yield steadily decreased with increasing pH (Table S5). Phototransformation of lamivudine in wetland water was fully inhibited by sorbic acid, histidine, and IPA but was unaltered in the presence of DMA (Figure S7). This indicates the importance of ³DOM*, $^1\text{O}_2$, and OH radicals for its indirect phototransformation. For emtricitabine, phototransformation rates in wetland water were affected only by IPA and sorbic acid (Figure S8), suggesting that reactions with $^1\text{O}_2$ are less important for this compound. The high photostability of its associated DNA base cytosine and nucleotide cytidine revealed the importance of structural modifications [thiol group (both compounds) and fluorine (emtricitabine)] to the observed photodegradation.

Additional experiments with individual reactive species revealed second-order reaction rates with $\bullet\text{OH}$ at or above (abacavir, zidovudine) diffusion-controlled rates ranging from 5×10^9 to $1.1 \times 10^{11} \text{ M}^{-1}\text{s}^{-1}$ (Table 1). Antiviral compounds were reactive with $\text{CO}_3^{\bullet-}$ at rates between 1.2×10^6 and $1.2 \times 10^9 \text{ M}^{-1}\text{s}^{-1}$, while only abacavir ($1.2 \times 10^9 \text{ M}^{-1}\text{s}^{-1}$) and acyclovir ($1.2 \times 10^7 \text{ M}^{-1}\text{s}^{-1}$) reacted with $^1\text{O}_2$. With the exception of abacavir, no depletion of antiviral compounds was observed in the presence of the model triplet photosensitizer 3MAP. However, depletion of all compounds was observed in the presence of AQ2S at rates similar to or higher than the reference probe compound trimethylphenol (TMP), indicating selective reactivity with excited triplet states. Comparison of measured and predicted rate constant for antivirals under wetland conditions (obtained by multiplication of steady-state concentrations of reactive species measured in wetland water

with measured second-order reaction rate constants of antivirals with $^1\text{O}_2$, $\bullet\text{OH}$, and $\bullet\text{CO}_3^-$) were in good agreement, indicating reasonable results.

Comparison of Photo- versus Biotransformation Rates. Dark experiments conducted with wetland water in the presence of biomat material indicated that biotransformation rates varied considerably among antiviral drugs. Biotransformation half-lives ($t_{1/2,\text{bio}}$) ranged from 74 h for acyclovir to 500 h (21 days) for emtricitabine (Figure 3; Figure S13).

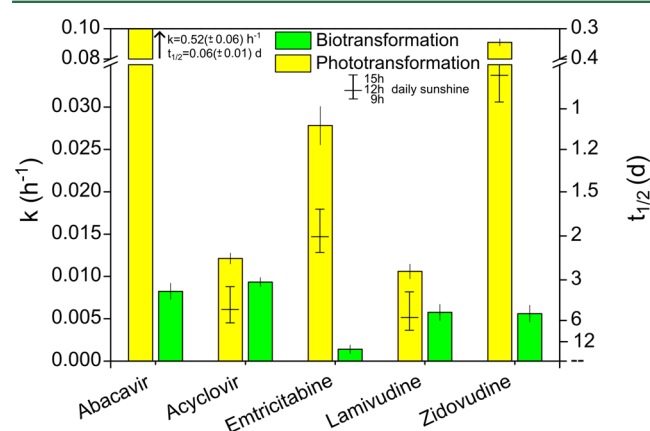


Figure 3. Photo- and biotransformation rate constants k (per hour) and associated half-life $t_{1/2}$ (days) of antiviral drugs in laboratory experiments. Small bars within phototransformation columns indicate half-lives based on daily sunshine hours (9–15 h). For determination of biodegradation half-lives, experiments were conducted in the presence of the biomat in the dark. Error bars represent 95% confidence intervals obtained from linear regressions.

Under typical wetland treatment conditions (i.e., hydraulic retention times of 2–3 days), significant biological attenuation of acyclovir and abacavir is expected, whereas removal of the other antiviral drugs via microbial processes is unlikely to be important. Comparison of transformation rates of antiviral drugs in the dark to those observed in irradiated wetland water indicated that phototransformation processes were dominant for abacavir, zidovudine, and emtricitabine, while for acyclovir and lamivudine, biotransformation was similar or more important than photolysis during typical summertime conditions (Figure 3).

Transformation of Abacavir. HRMS analysis indicated that four primary transformation products (TP318, TP288, TP284, and TP246) were formed during photolysis of abacavir in wetland water (Supporting Information section 2.2; Table

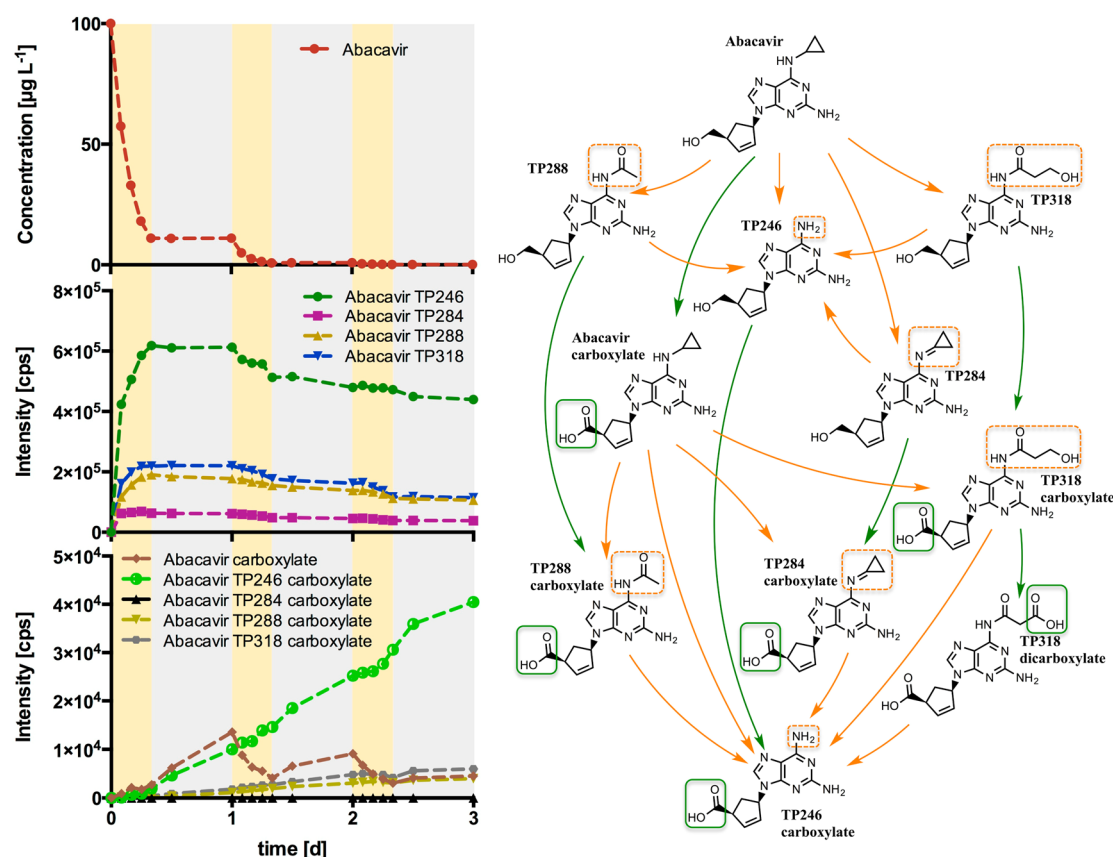


Figure 4. Transformation of abacavir (left, top) and resulting formation of photo-TPs (left, middle) and bio/bio-photo-TPs (left, bottom), as well as proposed transformation pathway (right), in combined 3-day experiments in the presence of biomat with 8 h of daily irradiation. In the transformation pathway, photo- and biotransformation reactions and structural changes in the molecules are indicated in orange and green, respectively.

S7). In agreement with results obtained for the structural analogues 2-aminoadenosine and adenine, fragmentation patterns of TP318, TP288, and TP246 revealed that the cyclopropylamine moiety was the main site of reaction, leaving the 2-aminoadenine (fragments m/z 151.073, 134.046, and 109.051) and the 2-cyclopenten-1-methanyl moieties (fragments m/z 95.353 and 79.054) unaltered.

Exact mass calculations of TP318 showed addition of two oxygen atoms to the cyclopropyl moiety ($\Delta m + 31.9898$ Da). Results from MS² experiments were consistent with scission of the cyclopropyl ring and the presence of a terminal hydroxyl group, as indicated by the cleavage of H₂O and CH₂O.

For TP288, MS data suggested modification of the cyclopropyl moiety via loss of one carbon atom and addition of one oxygen atom, leading to the formation of an acetamide, whereas TP246 was formed via cleavage of the cyclopropyl ring. The chemical structure of TP246 was confirmed by comparison with a commercially available reference standard. The exact mass and fragmentation pattern of TP284 was consistent with loss of two protons from either the cyclopropylamine or the 2-aminoadenosine moiety (fragments m/z 149.069 and 189.088 instead of m/z 151.073 and 191.104 compared to abacavir and the other TPs). When the high photolability of the cyclopropyl moiety is considered, these structural changes were most likely due to formation of a cyclopropylimine.

To assess the relative importance of direct and different indirect photolysis processes in formation of the observed abacavir transformation products, their formation was inves-

tigated in buffered water (direct photolysis only), wetland water (direct and indirect photolysis), and wetland water in the presence of different reactive intermediate scavengers. The results revealed that both direct and indirect photolysis of abacavir produced the same suite of TPs at similar relative concentrations, despite the fact that disappearance of the parent compound was significantly accelerated in the presence of DOM and individual reactive intermediates (Figures S17 and S18). Similar results have been reported for irgarol, an algacide that is structurally similar to abacavir, suggesting that the cyclopropylamine moiety is the main site of reaction under all conditions.³⁰ Photodegradation experiments in buffered ultrapure water with different optical filters indicated that wavelengths below 320 nm preferentially led to cleavage of the cyclopropyl moiety (TP246), whereas wavelengths above 320 nm (UVA and visible light) led to scission of the cyclopropyl ring followed by partial oxidation (TP318) (Figure S19).

These findings suggest that phototransformation of abacavir is initiated by a one-electron oxidation of the cyclopropylamine moiety, leading to formation of a cyclopropylaminium radical cation,^{31,32} followed by subsequent reactions resulting in formation of various products. Interestingly, this phenomenon has also been utilized for the investigation of electron-hopping in DNA by modifying guanine and adenine with cyclopropyl moieties.^{33,34} Due to the instability of the initially formed closed ring radical cation, the modification results in rapid cyclopropyl ring opening as well as 1,2-hydrogen migration,

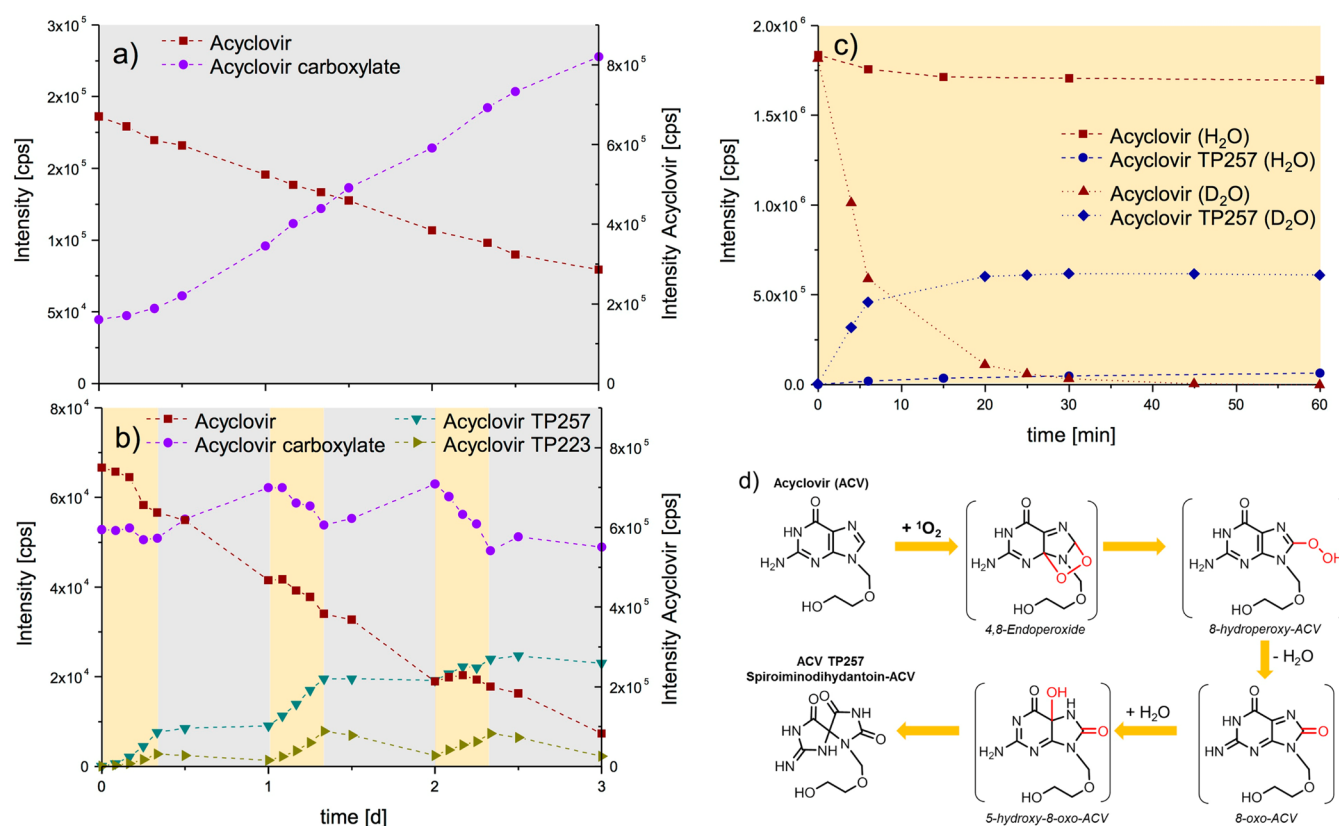


Figure 5. Transformation of acyclovir in the presence of biomat in the dark (a) and in combined photo- and biotransformation experiments (b), as well as formation of TP257 via reaction of acyclovir with 1O_2 in D_2O and H_2O by use of rose bengal as photosensitizer (c) and its proposed phototransformation pathway (d). Occurrence of acyclovir carboxylate at t_0 in panels a and b is due to its emission by the wastewater treatment plant that feeds the wetland.

leading to formation of an ionized allylamine.^{31,35} Scission of the ring is followed either by complete cleavage of the cyclopropyl moiety (TP246) or by reaction of the ring-opened radical cation with H_2O/O_2 .^{33,35} In the latter case, electron release from the carbon-centered radical followed by hydrolysis leads to formation of a 3-hydroxypropanaminium cation,³⁶ and subsequent addition of water results in formation of a 3-hydroxypropanamide (TP318). In our system, TP288 is formed by photolytic cleavage of the hydroxymethyl group, which leads to the formation of the acetamide product.^{36,37} TP284 was most likely formed via H-atom abstraction, resulting in formation of a neutral cyclopropyl radical, followed by an electron-transfer reaction and/or hydrolysis and elimination of water, even though this reaction has only been shown to be catalyzed by enzymes so far.^{38,39}

Experiments with biomat material in the dark to determine the relative importance of biotransformation reactions indicated that microbial transformation of abacavir mainly occurred via oxidation of the primary alcohol group of the 2-cyclopenten-1-hydroxymethyl side chain to produce the corresponding carboxylic acid (abacavir carboxylate, Figure S13). This was consistent with previous experiments conducted with mixed liquor-suspended solids from an activated sludge treatment plant.⁴⁰

When abacavir was exposed simultaneously to light and microorganisms (Figure 4), a rapid loss of the compound was observed during the first 8-h light period (i.e., initial concentration decreased by approximately 90%). For the next 16 h (i.e., the dark period), abacavir removal was significantly

slower. When the light was turned back on, nearly all remaining abacavir disappeared. As expected, the light-induced transformation of abacavir gave rise to the four photo-TPs described above (see middle panel of Figure 4). The concentrations of these photo-TPs decreased by approximately 25% over the next 2.5 days, indicating that further transformation took place, via either photolytic or microbial processes.

Additional biodegradation experiments with the four photo-TPs of abacavir revealed that biotransformation occurs at the same moiety as observed for the parent compound, leading to the corresponding TP246, TP284, TP288, and TP318 carboxylates (Figure S20). Exact mass data and fragmentation patterns of biophoto-TPs determined by HRMS analysis are included in Supporting Information section 2.2. Consequently, the observed decrease in concentration of photo-TPs shown in the middle panel of Figure 4 was mainly attributable to biotransformation, leading to a steady formation of carboxylate photo-TPs (bottom panel of Figure 4). Faster transformation rates of abacavir photo-TPs observed during irradiation periods may have been attributable to enhanced biotransformation due to elevated oxygen concentrations or elevated pH values that occurred when photosynthetic microbes in the biomat were active. Differences in biotransformation rates of TP246, TP284, TP288, and TP318, compared to abacavir (Figure S14), indicate that alteration of chemical structure influences biotransformation kinetics, for example, by affecting enzyme binding affinities or steric properties. Light exposure of abacavir carboxylate formed in the dark led to its phototransformation, ultimately yielding the same photo-TPs as abacavir (bottom

panel of Figure 4). When it is considered that abacavir is already transformed extensively to abacavir carboxylate in activated sludge treatment,⁴⁰ rapid elimination of both compounds can be expected in open-water unit process wetlands. In contrast to biotransformation reactions, similar phototransformation kinetics were observed for abacavir and abacavir carboxylate (Figure S12). TP246 carboxylate was identified as the main product that accumulates over time because it is not susceptible to further reactions.

Transformation of Acyclovir. In contrast to abacavir, the transformation of acyclovir was dominated by microbial processes (Figure 5), with biotransformation resulting in the formation of acyclovir carboxylate, which was not susceptible to further microbial transformation. These results are consistent with previous biotransformation experiments conducted with acyclovir in sewage sludge.⁴¹

In the absence of biomat material, exposure of wetland water to simulated sunlight resulted in formation of two main photo-TPs (TP257 and TP223). HRMS analysis indicated that TP257 contains two additional oxygen atoms on the guanine moiety, as evidenced by detection of fragment m/z 184 instead of m/z 152 (Table S8; Figure S16). Photosensitized degradation of guanine and guanosine occurs by reaction with excited triplet states, $^1\text{O}_2$, $\cdot\text{OH}$, or $\cdot\text{CO}_3^-$.^{42,43} The main product of reaction of guanine with $^1\text{O}_2$ has been identified as spiroiminodihydantoin.^{44–46} To assess the role of $^1\text{O}_2$ in the phototransformation of acyclovir in wetland water, experiments were conducted in both H_2O and D_2O in the presence of the $^1\text{O}_2$ sensitizer rose bengal (Figure 5). Lifetimes of $^1\text{O}_2$ in D_2O are more than an order of magnitude higher than in H_2O ,³⁹ and faster transformation of acyclovir in D_2O confirmed the role of $^1\text{O}_2$ in the indirect photolysis of acyclovir. In addition, the yield of TP257 increased in D_2O . Due to its photochemical properties, acyclovir is likely to undergo self-sensitization via photoexcitation and subsequent formation of $^1\text{O}_2$ as shown for guanine and guanosine.^{48–50} For the second acyclovir photo-TP (TP223), HRMS analysis indicated the loss of two protons, most likely from the side chain, as evidenced by the detection of fragments m/z 152, 135, and 110, suggesting that the guanine moiety remained unchanged (Table S8). Additional information obtained from fragmentation of the side chain was inconclusive but indicated oxidation of the terminal alcohol to the corresponding aldehyde via reaction with $\cdot\text{OH}$.⁵¹

Results from the 72-h simulated sunlight experiments conducted in the presence of the biomat revealed a steady decrease of acyclovir during light and dark periods, indicating the dominance of biotransformation processes (Figure 5b). However, biotransformation of acyclovir was significantly faster in the sunlight experiments compared to dark controls (Figure 5a,b), suggesting that the higher oxygen concentrations and elevated pH values that occurred when microorganisms in the biomat were undergoing photosynthesis played a role in biotransformation processes.¹⁰ In the presence of simulated sunlight, production of two phototransformation products (i.e., TP257 and TP224) was observed. No significant removal of TP257 was detected during dark periods, suggesting limited biotransformation via oxidation of the terminal hydroxyl group of the side chain. Although the exact reason for this is unknown, a plausible explanation is that structural modifications of the guanine core moiety prevented enzymatic oxidation of TP257. In contrast, concentrations of TP223 decreased in the dark. For the biotransformation product (i.e., acyclovir carboxylate), increasing concentrations were observed only

during dark periods, whereas its concentration decreased upon exposure to sunlight. This indicates that the compound was transformed further by photolytic processes, most likely via the same mechanisms as acyclovir. This was confirmed by additional irradiation experiments with acyclovir carboxylate in wetland water (results not shown).

Transformation of Zidovudine, Lamivudine, and Emtricitabine. Mass spectra of the phototransformation products of emtricitabine, lamivudine, and zidovudine indicated structural changes at different positions on the molecules (Tables S9–S11). For lamivudine and emtricitabine, HRMS analysis revealed oxidation of the riboside moiety (lamivudine TP245 and emtricitabine TP263), most likely via S-oxidation. This was confirmed by comparison with commercially available reference standards. Addition of H_2O to the 5-fluorocytosine moiety was observed for emtricitabine (emtricitabine TP265). Experiments conducted with the fluorine-free analogue lamivudine illustrate the importance of fluorine substitution: the F-moiety increases light absorbance at wavelengths >300 nm (Figure S2) for emtricitabine and leads to faster photodegradation (Figure 2, Table S5). Emtricitabine TP265 was formed via hydration of the double bond of the 5-fluorocytosine moiety, yielding a hydroxyl group at position C6. For zidovudine, observed phototransformations were mainly attributable to the photolability of the azido moiety. Formation of zidovudine TP239 can be explained by cleavage of N_2 , yielding a nitrene intermediate, which reacts further via intramolecular C–H insertion to an aziridine.^{52,53} Subsequent nucleophilic attack of the aziridine by water leads to hydroxylation of the C atom in β -position or formation of a hydroxylamine (zidovudine TP257).^{52,54} Results from HRMS analysis of zidovudine TP221 were inconclusive but indicated cleavage of N_2 and H_2O from the furanosyl moiety.

In addition, photolytic cleavage of the nitrogen–carbon bond between DNA base moieties and riboside analogue side chains was observed for all three compounds, resulting in formation of 5-fluorocytosine (emtricitabine TP129), cytosine (lamivudine TP111), and thymine (zidovudine TP126). None of these TPs was detected in sunlight experiments in the presence of biomat (Figures S21 and 22), indicating that they were rapidly transformed, most likely via microbial processes. For zidovudine, this was confirmed by additional biodegradation experiments with photo-TPs (thymine, TP239, and TP257), showing the rapid elimination of thymine (Figure S22). When the importance of both thymine and cytosine as DNA building blocks is considered, it is likely that they were incorporated into the microbial biomass. The fate of 5-fluorocytosine remains unclear.

Similar to abacavir and acyclovir, biotransformation of emtricitabine, lamivudine, and zidovudine was shown to result in the formation of carboxylated TPs via oxidation of the terminal alcohol as observed previously for abacavir and acyclovir (Figure S13). As carboxylated TPs are expected to follow the same phototransformation mechanisms as the parent compounds, the interaction of photo- and biotransformation reactions is likely to result in their complete elimination via mineralization and/or microbial uptake (Figure 6).

Environmental Implications. Differences between kinetics and transformation product formation in the presence and absence of the biomat highlight the complexity of transformation reactions that lead to the removal of trace organic contaminants in open-water unit process wetlands and other sunlit waters. Attempts to predict the environmental fate

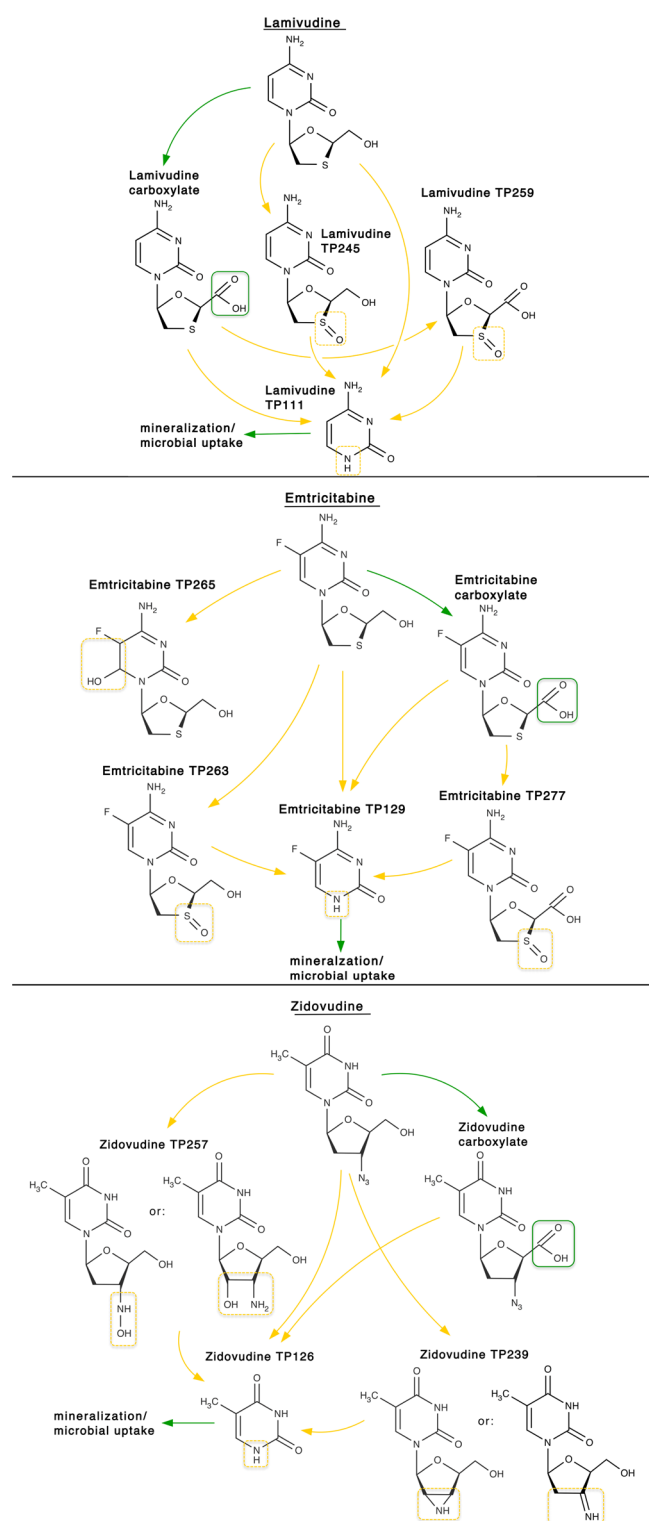


Figure 6. Proposed photo- and biodegradation pathway of lamivudine (top), emtricitabine (middle), and zidovudine (bottom) in open-water wetland cells. Orange and green arrows indicate photo- and biotransformation reactions, respectively.

of organic contaminants in these systems require an understanding of both processes as well as their potential interactions.

Identification of TPs showed that bio- and phototransformation reactions took place at different positions of the antiviral molecules. Phototransformation of biodegradation products

was found to occur at the same location as in the parent compound. As a result, mechanisms and kinetics were similar to those observed for parent antiviral compounds. This is important because carboxylate biodegradation products are typically present in much higher concentrations in biological treated wastewater compared to parent compounds.⁴⁰ In contrast, biodegradation kinetics of phototransformation products of antiviral drugs differed substantially from that observed for the parent compound even though the site of enzymatic oxidation did not change. This can be explained by differences in enzyme affinities and steric hindrance. For example, phototransformation of acyclovir created a transformation product (TP257) that was not susceptible to biotransformation by microorganisms that could oxidize the parent compound in the dark.

Combining kinetic studies with investigations of transformation product formation provides a better understanding of mechanisms relevant for the removal of trace organic contaminants in sunlit waters. By conducting biotransformation studies in the presence and absence of light, it is possible to assess interactions between transformation processes and the likelihood that complete mineralization of trace organic contaminants will occur. These data also suggest that relative ratios of antiviral compounds and their transformation products might be useful as in situ probes to assess the relative importance of microbial and photochemical transformation pathways. This study highlights the need to consider the formation of different transformation products in sunlit and light-shaded systems and the possibility of using knowledge of the reactivity of specific moieties in chemical fate assessment. When the variety of formed transformation products is considered, there is a need for appropriate risk assessment tools to assess potential adverse effects of transformation products with unknown toxicities on aquatic ecosystems. Additional field studies may further confirm these laboratory microcosm results and help to assess the suitability of approaches for determining the relative importance of individual transformation processes.

■ ASSOCIATED CONTENT

📄 Supporting Information

The Supporting Information is available free of charge on the ACS Publications website at DOI: 10.1021/acs.est.5b03783.

Additional text, 22 figures, and 16 tables with information on sample analysis, UV spectra of antiviral drugs, phototransformation kinetics plots, determination of indirect photolysis reaction rate constants, quantum yields, steady-state concentrations of reactive intermediates in wetland water, experiments with DNA model compounds, MSⁿ fragments of transformation products, formation and fate of abacavir photo-TPs by different reactive intermediates, and results of combined bio- and phototransformation experiments with emtricitabine, lamivudine and zidovudine (PDF)

■ AUTHOR INFORMATION

Corresponding Author

*E-mail sedlak@berkeley.edu.

Notes

The authors declare no competing financial interest.

ACKNOWLEDGMENTS

C.P. by a postdoctoral scholarship of the German Academic Exchange Service (DAAD). J.W. was supported by a scholarship of the Swiss National Science Foundation (PBEZP2-142887). Financial support by the Engineering Research Center for Reinventing the Nation's Water Infrastructure (ReNUWit) EEC-1028968, and TransRisk, funded by the German Ministry of Science and Education, is gratefully acknowledged.

REFERENCES

- (1) Burrows, H. D.; Canle, M.; Santaballa, J. A.; Steenken, S. Reaction pathways and mechanisms of photodegradation of pesticides. *J. Photochem. Photobiol., B* **2002**, *67* (2), 71–108.
- (2) Boreen, A. L.; Arnold, W. A.; McNeill, K. Photodegradation of pharmaceuticals in the aquatic environment: A review. *Aquat. Sci.* **2003**, *65* (4), 320–341.
- (3) Halling-Sorensen, B.; Nielsen, S. N.; Lanzky, P. F.; Ingerslev, F.; Lutzhoft, H. C. H.; Jorgensen, S. E. Occurrence, fate and effects of pharmaceutical substances in the environment - A review. *Chemosphere* **1998**, *36* (2), 357–393.
- (4) Onesios, K. M.; Yu, J. T.; Bouwer, E. J. Biodegradation and removal of pharmaceuticals and personal care products in treatment systems: a review. *Biodegradation* **2009**, *20* (4), 441–466.
- (5) Lam, M. W.; Mabury, S. A. Photodegradation of the pharmaceuticals atorvastatin, carbamazepine, levofloxacin, and sulfamethoxazole in natural waters. *Aquat. Sci.* **2005**, *67* (2), 177–188.
- (6) Chiron, S.; Minero, C.; Vione, D. Photodegradation processes of the antiepileptic drug carbamazepine, relevant to estuarine waters. *Environ. Sci. Technol.* **2006**, *40* (19), 5977–5983.
- (7) De Laurentiis, E.; Chiron, S.; Kouras-Hadef, S.; Richard, C.; Minella, M.; Maurino, V.; Minero, C.; Vione, D. Photochemical fate of carbamazepine in surface freshwaters: Laboratory measures and modeling. *Environ. Sci. Technol.* **2012**, *46* (15), 8164–8173.
- (8) Kaiser, E.; Prasse, C.; Wagner, M.; Broeder, K.; Ternes, T. A. Transformation of oxcarbazepine and human metabolites of carbamazepine and oxcarbazepine in wastewater treatment and sand filters. *Environ. Sci. Technol.* **2014**, *48* (17), 10208–10216.
- (9) Jasper, J. T.; Nguyen, M. T.; Jones, Z. L.; Ismail, N. S.; Sedlak, D. L.; Sharp, J. O.; Luthy, R. G.; Horne, A. J.; Nelson, K. L. Unit process wetlands for removal of trace organic contaminants and pathogens from municipal wastewater effluents. *Environ. Eng. Sci.* **2013**, *30* (8), 421–436.
- (10) Jasper, J. T.; Sedlak, D. L. Phototransformation of wastewater-derived trace organic contaminants in open-water unit process treatment wetlands. *Environ. Sci. Technol.* **2013**, *47* (19), 10781–10790.
- (11) Nguyen, M. T.; Silverman, A. I.; Nelson, K. L. Sunlight inactivation of MS2 coliphage in the absence of photosensitizers: Modeling the endogenous inactivation rate using a photoaction spectrum. *Environ. Sci. Technol.* **2014**, *48* (7), 3891–3898.
- (12) Silverman, A. I.; Nguyen, M. T.; Schilling, I. E.; Wenk, J.; Nelson, K. L. Sunlight inactivation of viruses in open-water unit process treatment wetlands: Modeling endogenous and exogenous inactivation rates. *Environ. Sci. Technol.* **2015**, *49* (5), 2757–2766.
- (13) Jasper, J. T.; Jones, Z. L.; Sharp, J. O.; Sedlak, D. L. Biotransformation of trace organic contaminants in open-water unit process treatment wetlands. *Environ. Sci. Technol.* **2014**, *48* (9), 5136–5144.
- (14) Jasper, J. T.; Jones, Z. L.; Sharp, J. O.; Sedlak, D. L. Nitrate removal in shallow, open-water treatment wetlands. *Environ. Sci. Technol.* **2014**, *48* (19), 11512–11520.
- (15) Wood, T. P.; Duvenage, C. S. J.; Rohwer, E. The occurrence of anti-retroviral compounds used for HIV treatment in South African surface water. *Environ. Pollut.* **2015**, *199*, 235–243.
- (16) Peng, X.; Wang, C.; Zhang, K.; Wang, Z. F.; Huang, Q. X.; Yu, Y. Y.; Ou, W. H. Profile and behavior of antiviral drugs in aquatic environments of the Pearl River Delta, China. *Sci. Total Environ.* **2014**, *466*, 755–761.
- (17) Prasse, C.; Schluesener, M. P.; Schulz, R.; Ternes, T. A. Antiviral drugs in wastewater and surface waters: A new pharmaceutical class of environmental relevance? *Environ. Sci. Technol.* **2010**, *44* (5), 1728–1735.
- (18) Azuma, T.; Nakada, N.; Yamashita, N.; Tanaka, H. Synchronous dynamics of observed and predicted values of anti-influenza drugs in environmental waters during a seasonal influenza outbreak. *Environ. Sci. Technol.* **2012**, *46* (23), 12873–12881.
- (19) Wommack, K. E.; Colwell, R. R. Virioplankton: Viruses in aquatic ecosystems. *Microbiol. Mol. Biol. R.* **2000**, *64* (1), 69–114.
- (20) Dulin, D.; Mill, T. Development and evaluation of sunlight actinometers. *Environ. Sci. Technol.* **1982**, *16* (11), 815–820.
- (21) Grebel, J. E.; Pignatello, J. J.; Mitch, W. A. Sorbic acid as a quantitative probe for the formation, scavenging and steady-state concentrations of the triplet-excited state of organic compounds. *Water Res.* **2011**, *45* (19), 6535–6544.
- (22) Boreen, A. L.; Edlund, B. L.; Cotner, J. B.; McNeill, K. Indirect photodegradation of dissolved free amino acids: The contribution of singlet oxygen and the differential reactivity of DOM from various sources. *Environ. Sci. Technol.* **2008**, *42* (15), 5492–5498.
- (23) Packer, J. L.; Werner, J. J.; Latch, D. E.; McNeill, K.; Arnold, W. A. Photochemical fate of pharmaceuticals in the environment: Naproxen, diclofenac, clofibric acid, and ibuprofen. *Aquat. Sci.* **2003**, *65* (4), 342–351.
- (24) Vione, D.; Khanra, S.; Man, S. C.; Maddigapu, P. R.; Das, R.; Arsene, C.; Olariu, R.-I.; Maurino, V.; Minero, C. Inhibition vs. enhancement of the nitrate-induced phototransformation of organic substrates by the (OH)-O-center dot scavengers bicarbonate and carbonate. *Water Res.* **2009**, *43* (18), 4718–4728.
- (25) Canonica, S.; Kohn, T.; Mac, M.; Real, F. J.; Wirz, J.; Von Gunten, U. Photosensitizer method to determine rate constants for the reaction of carbonate radical with organic compounds. *Environ. Sci. Technol.* **2005**, *39* (23), 9182–9188.
- (26) Bedini, A.; De Laurentiis, E.; Sur, B.; Maurino, V.; Minero, C.; Brigante, M.; Mailhot, G.; Vione, D. Phototransformation of anthraquinone-2-sulphonate in aqueous solution. *Photochem. Photobiol. S.* **2012**, *11* (9), 1445–1453.
- (27) Zepp, R. G.; Hoigne, J.; Bader, H. Nitrate-induced photo-oxidation of trace organic chemicals in water. *Environ. Sci. Technol.* **1987**, *21*, 443–450.
- (28) Burns, J. M.; Cooper, W. J.; Ferry, J. L.; King, D. W.; DiMento, B. P.; McNeill, K.; Miller, C. J.; Miller, W. L.; Peake, B. M.; Rusak, S. A.; Rose, A. L.; Waite, T. D. Methods for reactive oxygen species (ROS) detection in aqueous environments. *Aquat. Sci.* **2012**, *74* (4), 683–734.
- (29) Maddigapu, P. R.; Bedini, A.; Minero, C.; Maurino, V.; Vione, D.; Brigante, M.; Mailhot, G.; Sarakha, M. The pH-dependent photochemistry of anthraquinone-2-sulfonate. *Photochem. Photobiol. Sci.* **2010**, *9* (3), 323–330.
- (30) Sakkas, V. A.; Lambropoulou, D. A.; Albanis, T. A. Photochemical degradation study of irgarol 1051 in natural waters: influence of humic and fulvic substances on the reaction. *J. Photochem. Photobiol., A* **2002**, *147* (2), 135–141.
- (31) Bouchoux, G.; Alcaraz, C.; Dutuit, O.; Nguyen, M. T. Unimolecular chemistry of the gaseous cyclopropylamine radical cation. *J. Am. Chem. Soc.* **1998**, *120* (1), 152–160.
- (32) Cooksy, A. L.; King, H. F.; Richardson, W. H. Molecular orbital calculations of ring opening of the isoelectronic cyclopropylcarbonyl radical, cyclopropoxy radical, and cyclopropylaminium radical cation series of radical clocks. *J. Org. Chem.* **2003**, *68* (24), 9441–9452.
- (33) Nakatani, K.; Dohno, C.; Saito, I. Design of a hole-trapping nucleobase: Termination of DNA-mediated hole transport at N-2-cyclopropyldeoxyguanosine. *J. Am. Chem. Soc.* **2001**, *123* (39), 9681–9682.
- (34) Shao, F. W.; O'Neill, M. A.; Barton, J. K. Long-range oxidative damage to cytosines in duplex DNA. *Proc. Natl. Acad. Sci. U. S. A.* **2004**, *101* (52), 17914–17919.

- (35) Qin, X. Z.; Williams, F. Electron-spin-resonance studies on the radical cation mechanism of the ring-opening of cyclopropylamines. *J. Am. Chem. Soc.* **1987**, *109* (2), 595–597.
- (36) Paul, M. M. S.; Aravind, U. K.; Pramod, G.; Saha, A.; Aravindakumar, C. T. Hydroxyl radical induced oxidation of theophylline in water: a kinetic and mechanistic study. *Org. Biomol. Chem.* **2014**, *12* (30), 5611–5620.
- (37) Goutailler, G.; Valette, J. C.; Guillard, C.; Paise, O.; Faure, R. Photocatalysed degradation of cyromazine in aqueous titanium dioxide suspensions: comparison with photolysis. *J. Photochem. Photobiol., A* **2001**, *141* (1), 79–84.
- (38) Shaffer, C. L.; Morton, M. D.; Hanzlik, R. P. N-dealkylation of an N-cyclopropylamine by horseradish peroxidase. Fate of the cyclopropyl group. *J. Am. Chem. Soc.* **2001**, *123* (35), 8502–8508.
- (39) Cerny, M. A.; Hanzlik, R. P. Cytochrome P450-catalyzed oxidation of N-benzyl-N-cyclopropylamine generates both cyclopropanone hydrate and 3-hydroxypropionaldehyde via hydrogen abstraction, not single electron transfer. *J. Am. Chem. Soc.* **2006**, *128* (10), 3346–3354.
- (40) Funke, J.; Prasse, C.; Ternes, T. A. Identification and fate of transformation products of antiviral drugs formed during biological wastewater treatment (submitted for publication).
- (41) Prasse, C.; Wagner, M.; Schulz, R.; Ternes, T. A. Biotransformation of the antiviral drugs acyclovir and penciclovir in activated sludge treatment. *Environ. Sci. Technol.* **2011**, *45* (7), 2761–2769.
- (42) Cadet, J.; Douki, T.; Gasparutto, D.; Ravanat, J. L. Oxidative damage to DNA: formation, measurement and biochemical features. *Mutat. Res., Fundam. Mol. Mech. Mutagen.* **2003**, *531* (1–2), 5–23.
- (43) Neeley, W. L.; Essigmann, J. M. Mechanisms of formation, genotoxicity, and mutation of guanine oxidation products. *Chem. Res. Toxicol.* **2006**, *19* (4), 491–505.
- (44) Cui, L.; Ye, W.; Prestwich, E. G.; Wishnok, J. S.; Taghizadeh, K.; Dedon, P. C.; Tannenbaum, S. R. Comparative analysis of four oxidized guanine lesions from reactions of DNA with peroxynitrite, singlet oxygen and γ -radiation. *Chem. Res. Toxicol.* **2013**, *26* (2), 195–202.
- (45) Luo, W.; Muller, J. G.; Rachlin, E. M.; Burrows, C. J. Characterization of spiroiminodihydantoin as a product of one-electron oxidation of 8-oxo-7,8-dihydroguanosine. *Org. Lett.* **2000**, *2* (5), 613–616.
- (46) Cadet, J.; Douki, T.; Ravanat, J. L. Oxidatively generated damage to the guanine moiety of DNA: Mechanistic aspects and formation in cells. *Acc. Chem. Res.* **2008**, *41* (8), 1075–1083.
- (47) Rodgers, M. A. J.; Snowden, P. T. Lifetime of $O_2(1\Delta g)$ in liquid water as determined by time-resolved infrared luminescence measurements. *J. Am. Chem. Soc.* **1982**, *104* (20), 5541–5543.
- (48) Mohammad, T.; Morrison, H. Evidence for the photosensitized formation of singlet oxygen by UVB irradiation of 2'-deoxyguanosine 5'-monophosphate. *J. Am. Chem. Soc.* **1996**, *118* (5), 1221–1222.
- (49) Redmond, R. W.; Gamlin, J. N. A compilation of singlet oxygen yields from biologically relevant molecules. *Photochem. Photobiol.* **1999**, *70* (4), 391–475.
- (50) Torun, L.; Morrison, H. Photooxidation of 2'-deoxyguanosine 5'-monophosphate in aqueous solution. *Photochem. Photobiol.* **2003**, *77* (4), 370–375.
- (51) von Gunten, U. Ozonation of drinking water: Part I. Oxidation kinetics and product formation. *Water Res.* **2003**, *37* (7), 1443–1467.
- (52) Dunge, A.; Chakraborti, A. K.; Singh, S. Mechanistic explanation to the variable degradation behaviour of stavudine and zidovudine under hydrolytic, oxidative and photolytic conditions. *J. Pharm. Biomed. Anal.* **2004**, *35* (4), 965–970.
- (53) Gritsan, N.; Platz, M. Photochemistry of azides: The azide/nitrene interface. In *Organic Azides: Syntheses and Applications*; Bräse, S., Banert, K., Eds.; John Wiley & Sons: Chichester, U.K., 2010; Chapt. 11, pp 311–372; DOI: [10.1002/9780470682517.ch11](https://doi.org/10.1002/9780470682517.ch11).
- (54) Iwamoto, T.; Hiraku, Y.; Oikawa, S.; Mizutani, H.; Kojima, M.; Kawanishi, S. Oxidative DNA damage induced by photodegradation products of 3'-azido-3'-deoxythymidine. *Arch. Biochem. Biophys.* **2003**, *416* (2), 155–163.